

Fig. 1. Rate (in nanomoles per milligram of protein) of ethylene ( $C_2H_4$ ) and malonaldehyde formation by rat liver microsomes. The reaction system contained in a total volume of 5 ml (in  $\mu$ mole): tris buffer (pH 7.5), 50; KCl, 300; NADPH $_2$ , 0.6; ATP, 2.0; cupric ions, 5; and ascorbate, 50; in addition it contained 6 mg of microsomal protein. Microsomes were prepared as described by Ernster *et al.* (8). Arrows indicate further addition of 50  $\mu$ mole of ascorbate at times indicated. Malonaldehyde was determined by the thiobarbituric acid reaction (9); a molar extinction coefficient, at 535 m $\mu$ , of  $1.56 \times 10^5$  was used to determine malonaldehyde formed in the reaction (10). Ethylene was determined as previously described by Meigh *et al.* (11).

activity in animal systems. The dictates of comparative biochemistry suggest that if ethylene, in minute concentrations, possesses physiological activities in plant cells (1), it is feasible to consider that it may also affect animal cells.

MORRIS LIEBERMAN

*Pioneering Research Laboratory for Post Harvest Physiology, Agricultural Research Service, U.S. Department of Agriculture, Beltsville, Maryland*

PAUL HOCHSTEIN

*Department of Physiology and Pharmacology, Duke Medical Center, Durham, North Carolina*

#### References and Notes

1. S. Burg, *Ann. Rev. Plant Physiol.* **13**, 265 (1962).
2. M. Lieberman and L. W. Mapson, *Nature* **204**, 343 (1964).
3. P. Hochstein and L. Ernster, *Biochem. Biophys. Res. Commun.* **12**, 388 (1963).
4. P. Hochstein, K. Nordenbrand, L. Ernster, *ibid.* **14**, 323 (1964).
5. L. A. Witting, *Federation Proc.* **24**, 912 (1965).
6. G. Ram Chandra and M. Spencer, *Nature* **197**, 366 (1963).
7. C. N. Chipman, *Curr. Res. Anesth. Analg.* **10**, 206 (1931).
8. L. Ernster, P. Siekevitz, G. Palade, *J. Cell Biol.* **15**, 541 (1962).
9. F. Bernheim, M. L. Bernheim, K. M. Wilbur, *J. Biol. Chem.* **174**, 257 (1948).
10. R. O. Sinnhuber and T. C. Yo, *Food Res.* **23**, 626 (1958).
11. D. F. Meigh, K. H. Norris, C. C. Craft, M. Lieberman, *Nature* **186**, 902 (1960).
12. Supported in part by grants from NSF GB-1094 and GB-1416 and by PHS career award to P.H.

27 December 1965

## Nature of the Packing of Ribosomes within Chromatoid Bodies

**Abstract.** Optical Fourier transforms, made of electron micrographs of the crystalline array of ribonucleoprotein known as chromatoid bodies of *Entamoeba invadens*, have been interpreted as the transforms of a helix of 12 nodes in five turns. A model shows that this helix may be built of spheres 180 angstroms in diameter, placed at a radius of 150 angstroms. The optical transform of the model is very similar to the transform of the original electron micrograph.

Chromatoid bodies, so named because they stain with basic dyes, have been known to parasitologists as diagnostic features of several species of *Entamoeba* for 70 years. In *Entamoeba invadens*, the species we have studied, the bodies occur within the cysts as refractile rods, about  $3 \times 3 \times 8 \mu$  in size. Their nature was unknown until recently. In 1955 Pan and Gieman (1) were able to demonstrate the presence of RNA, but not DNA, within the bodies by histochemical tests. In 1958 Barker and Deutsch (2) reported that, in electron micrographs, these bodies consisted of crystalline arrays of particles  $\sim 200 \text{ \AA}$  in diameter. In further studies (3), Barker and Svihla were able to demonstrate that the ultraviolet absorption of the chromatoid bodies was consistent with a high RNA content, and they suggested the probable ribosomal nature of the  $\sim 200\text{-\AA}$  particles. In 1963 Siddiqui and Rudzinska (4) published electron micrographs showing a helical arrangement of the ribosomes in chromatoid bodies, but the details of the helix were not resolved. These authors pointed out that the hexagonally packed crystalline array seen in some sections must be the appearance of the chromatoid body when sectioned at right angles (cross sections) to the planes in which the helical arrays are disclosed (longitudinal sections).

Below we interpret fortunately oriented electron micrographs of sections through chromatoid bodies by the use of optical diffraction techniques. The combined use of these techniques was first described by Klug and Berger (5). From such data, we have been able to deduce the helical parameters which describe the packing of the ribosome particles within the chromatoid bodies.

Amoebas were cultivated as described

by Morgan and Terkelsen (6). Cysts were fixed for microscopy by the addition of glutaraldehyde (50-percent solution, Fisher) directly to the culture fluid. After being washed and postfixed in Dalton's chrome-osmium solution, the cells were stained with 1 percent uranyl acetate in 10 percent formalin. The preparations were then dehydrated in acetone, followed by immersion in propylene oxide and embedding in an Epon-Araldite mixture. Sections were cut with glass knives on LKB ultramicrotomes, stained with lead citrate, and examined in a Philips model 200 electron microscope. An example of a longitudinal section is shown in Fig. 1.

From such micrographs, various measurements (such as those of particle diameter and chain separation) may be made directly. Although a helical packing is strongly suggested, it is virtually impossible to follow the exact course of any one helix in such a picture. An objective method of analyzing all the regularities seen here involves taking the Fourier transform of the picture, and this may be done by using the micrograph as the "mask" (or "specimen") of the optical diffractometer.

Table 1. Layer line measurements from optical transform of Fig. 1.

Layer line assignments	Observed spacing* ( $\text{\AA}$ )	Calculated spacing for 900- $\text{\AA}$ period
2	432	450
3	308	300
5	180	180
7	127	129

\* Spacing calculated from measurements on the diffractogram, the optical constants of diffractometer, and the magnification of electron micrograph. The accuracy of these and other spacings given in the text is about  $\pm 5$  percent.

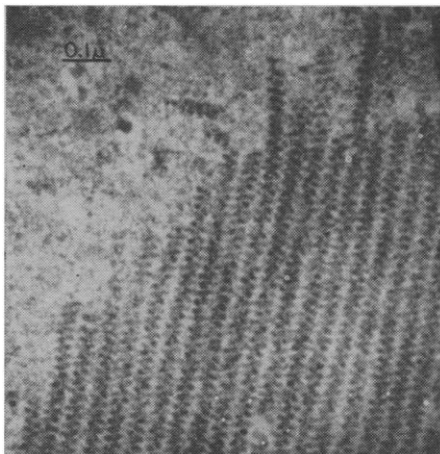


Fig. 1. Electron micrograph of a section through a chromatoid body of *Entamoeba invadens*. The distance between neighboring chains is 440  $\text{\AA}$ .

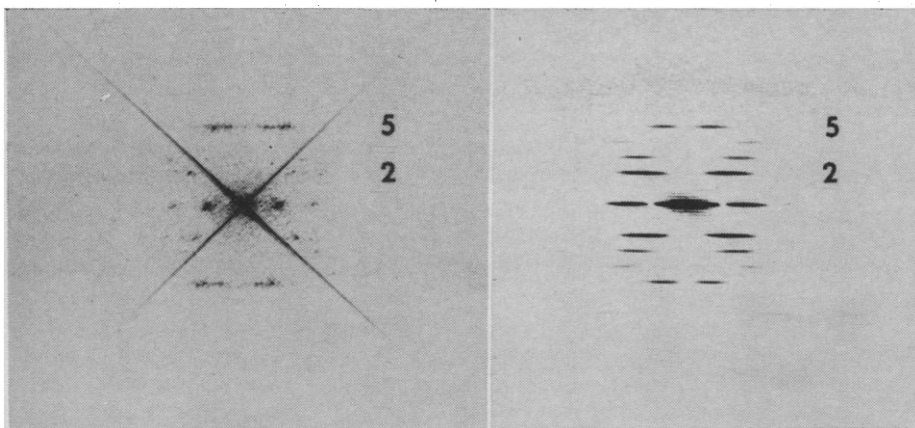


Fig. 2. (Left) Optical transform or diffractogram made directly from a negative of Fig. 1. The numbers give the assigned layer line indexing. Exposure time: 18 hours. The long-armed "X" through the center is the transform of the rectangular area of the mask which was exposed in the diffractometer, and is not due to any of the pattern within the electron micrograph itself. (Right) Diffractogram of a single helix, 12 nodes in five turns, five repeat periods long. Exposure time: 1 hour.

The diffractometer used was the one built and described by Wyckoff *et al.* (see 7). The optical transform (or "diffractogram") of Fig. 1 is shown in Fig. 2 (left), and may instantly be recognized as the transform of a helix. One has only to assign the correct orders to the Bessel functions involved in order to deduce the parameters of the helix (8). The layer line spacings seen and their indexing are given in Table 1. The helical repeat distance is 900 Å.

We assign the strong reflection on the fifth layer line to a first order Bessel function,  $J_1$ , since it is the nearest to the meridian but is clearly not truly meridional. Then the next strongest reflection, on the second layer line, which is also the next furthest from the meridian, must be a  $J_2$ . There is no other  $J_1$  on any layer line between 1 and 5. A very weak reflection on the seventh layer line could possibly be a  $J_1$ . The smallest set of helical parameters which will give such Bessel functions is provided by 12 scattering nodes in five turns. From the radius of the  $J_1$  on the fifth layer line (and knowing the magnification of the electron micrograph "mask"), we compute that the centers of about 150 Å from the helix axis. If we then identify a "scattering node" with one of the particles 180 Å in diameter (that is, ribosomes) seen in the micrographs, we can build an idealized model of a chromatoid body. Two helical units of such a model are shown in Fig. 3. The optical transform of the projection of one such unit onto a plane through the helical axis and including one node (made according to the tech-

nique given in Wyckoff *et al.*, 7) is shown in Fig. 2 (right). Although the intensities of the diffraction maxima given by this model do not exactly match those given by the micrograph (nor could they be expected to), the positions in reciprocal space of both sets of these maxima match very well. We take the goodness of this fit as an indication that we have correctly interpreted the helical parameters. The equator of the transform of the electron micrograph (Fig. 2, left) shows two reflections which are the first and second orders of 440 Å, the spacing between adjacent helices. These reflections are not seen in the transform of the model (Fig. 2, right) because it is the transform of only one helical unit.

The model places ribosomes on the helical net of 12 nodes in five turns, but we see that the resulting structure is more simply (and equivalently) visualized as being built of two opposing chains, each consisting of six ribosomes in one turn. One chain is carried into the other by a rotation of 150° and a translation of 75 Å about and along the helical axis. Along any one chain, ribosomal units 180 Å in diameter are in contact with each other. Neither the micrographs nor their diffraction patterns give any indication of more detailed structure within these apparently spherical units.

The fact that, at the edge of the chromatoid bodies, helices of ribosomes are seen both lying free in the neighboring cytoplasm and attached to the crystalline arrays at various angles, suggests the pre-assembly of the helices within the cytoplasm. If these helices consist only of spherical particles 180

Å in diameter, arranged, as in our model, with their centers at a radius of 150 Å, then there would exist an empty core, of radius 60 Å, down the middle of each double-helical strand. Since, in the micrographs, the electron density along any helical axis is obviously greater than the electron density between adjacent helices within the crystal, one can postulate the presence of some sort of core material filling this space.

Electron microscopy of other ribosomes has shown (9) that they consist of a larger (50S or 60S) and a smaller (30S or 40S) subunit. If we assume that our 180-Å particle represents the larger subunit, then there would be room within the proposed packing for the smaller subunits of one chain to bridge the gap across the helical axis and make contact with the smaller subunits of the ribosomes on the opposite chain. This type of dimerization has been seen previously in preparations of 100S particles (10).

It remains to be seen whether the forces involved in maintaining ribosomal units within an individual helix are significantly different from the forces involved in achieving crystalline coherence of neighboring helices. Experiments designed to elucidate these points are in progress and will be reported separately.

Electron micrographs of cross sections through the chromatoid bodies show that the helices are packed together on a hexagonal lattice with a separation between centers of approximately 440 Å. The proposed model accommodates such a packing, and suggests that neighboring chains will pack

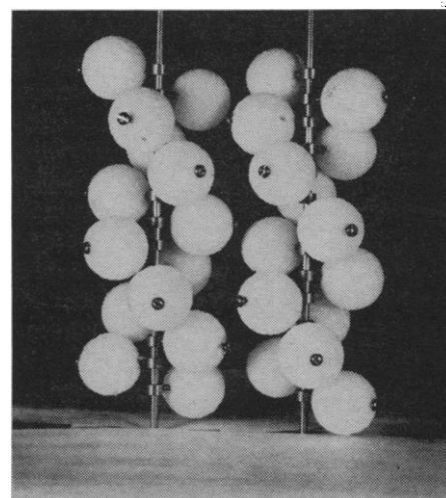


Fig. 3. Photograph of a model of two helices, each composed of 12 nodes (180 Å in diameter) in five turns. The separation between the helical axes is 440 Å.

more easily if displaced vertically with respect to one another by about one-sixth of the period. Inspection of Fig. 1 shows that this displacement is indeed seen in the micrographs.

RICHARD S. MORGAN  
BETTY G. UZMAN

Children's Cancer Research  
Foundation, Children's Hospital  
Medical Center, Boston, Massachusetts

#### References and Notes

1. C.-T. Pan and Q. M. Geiman, *Am. J. Hyg.* **62**, 66 (1955).
2. D. C. Barker and K. Deutsch, *Exptl. Cell Res.* **15**, 604 (1958).
3. D. C. Barker and G. Svihla, *J. Cell Biol.* **20**, 389 (1964).
4. W. A. Siddiqui and M. A. Rudzinska, *Nature* **200**, 74 (1963).
5. A. Klug and J. E. Berger, *J. Mol. Biol.* **10**, 565 (1964).
6. R. S. Morgan and K. Terkelsen, in preparation.
7. H. W. Wyckoff, R. S. Bear, R. S. Morgan, D. Carlstrom, *J. Opt. Soc. Am.* **47**, 1061 (1957).
8. W. Cochran, F. H. C. Crick, V. Vand, *Acta Cryst.* **5**, 581 (1952).
9. C. E. Hall and H. S. Slayter, *J. Mol. Biol.* **1**, 329 (1959).
10. H. E. Huxley and G. Zubay, *ibid.* **2**, 10 (1960).
11. We thank D. C. Barker for the strains and culture methods of *Entamoeba invadens*; A. Rich for the use of the optical diffractometer; our colleagues D. L. D. Caspar, C. Cohen, R. Langridge, W. Longley, G. Milman, and M. Sundaralingam for consultation; and Anja Mitchell, Patricia Hutchins, Eleanora Galvanek, and Ron MacNeil for technical assistance. Especial acknowledgement is made of the support of the director of research, Sidney Farber. This work was supported by grants from the legacy of Loula D. Lasker, New York City, the Albert and Mary Lasker Foundation, the NSF (GB 4238), General Research Support Funds, the Children's Cancer Research Foundation, and NIH (C 6516).

17 January 1966

## Visceral Reflex Activity: Development in Postnatal Rabbit

**Abstract.** In postnatal rabbits there is progressive development of central regulation of the micturition reflex. During the first 1 to 2 days of postnatal life a coordinated sustained reflex may be obtained from the bladder which has been isolated from the central nervous system. Changes in reflex integration occur over the following 7 to 12 days, which result in a coordinated reflex dependent upon supraspinal influences.

Stimulation and ablation studies have indicated the significance of specific brainstem and spinal cord areas in the regulation of the micturition reflex in mammals (1). Transection of the brainstem of the cat below the level of the rostral pons results in abolition of the high-amplitude, sustained, contractile response of the urinary bladder elicited by slow retrograde filling (2). This contractile response with sequential passive relaxation of the sphincter effects completes evacuation of the bladder. The ontogeny of this reflex has not been investigated. Forty-eight New Zealand rabbits ranging in age from 1 day to 6 months were studied (3). Rabbits were anesthetized with ether;

tracheostomy was performed, and a polyethylene catheter of appropriate size was inserted through the distal urethra into the bladder. The urethral catheter was connected to a T-shaped cannula; one arm of the "T" was connected to the output of a positive displacement pump (4) and the other arm to a strain gauge whose output was recorded on a Model 680 Moseley Autograf strip chart recorder. Warm, normal saline was pumped into the bladder slowly at known infusion rates. A cystometrogram and a determination of the reflex threshold and amplitude of the contractile response were made while the intact animal was under light ether anesthesia. A laminectomy was per-

formed and the spinal cord was transected either at the cervico-medullary junction or at the mid-thoracic level. Transection of the spinal cord was performed by suction ablation, and more cystometrograms were made. This procedure was followed by laminectomy and suction ablation of the lumbo-sacral portion of the spinal cord, after which a third set of cystometrograms were made. The animals were killed and autopsied, and completeness of spinal cord transection was checked. Results of these experiments are shown in Fig. 1.

In the first 1 to 2 days of postnatal life neither section of the cervical and thoracic cord nor destruction of the lumbo-sacral cord abolished the micturition reflex. To the contrary, the micturition reflex was frequently increased in amplitude after these procedures (5). From the 3rd to the 13th or 14th day of postnatal life the reflex was inconsistently abolished by transection of the spinal cord at the mid-thoracic level. Subsequent ablation of the lumbo-sacral cord at this time did not abolish the bladder contractile response in one of the two 10-day-old animals that we tested. After the 2nd week of postnatal life, transection of the spinal cord at either the cervico-medullary junction or the mid-thoracic portion of the spinal cord resulted in loss of the micturition reflex. No consistent change was observed in either low-amplitude vesical rhythmic activity or slope of the tonus limb after the ablation procedures throughout this interval.

Developmental studies of tonic postural mechanisms have indicated that maturational changes occur in the first 2 to 3 weeks of postnatal life in a cranio-caudal direction (6). These maturational changes are due to developmental changes in afferent reflex pathways. Studies in adult animals have indicated a close association between tonic postural mechanisms and micturition reflex threshold (7). A similar time course in developmental sequence of the micturition reflex and postural mechanisms would be anticipated. Our results confirm the similarity of temporal sequence in development of supraspinal regulation of the micturition reflex.

It is concluded from these experiments that the urinary bladder of the rabbit is in functional isolation from the central nervous system during the first 1 to 2 days of postnatal life. After this interval, activity of the bladder reflex is functionally integrated into the lumbo-sacral spinal cord. Following the

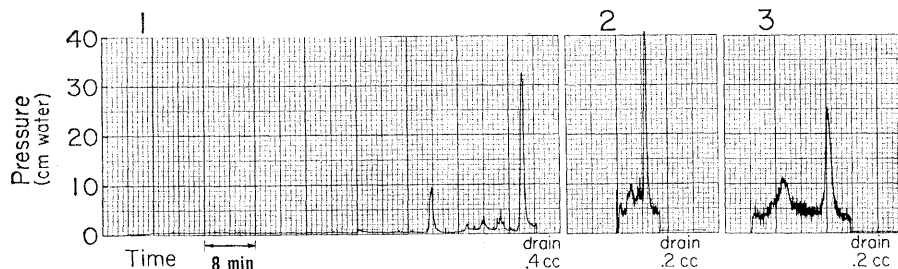


Fig. 1. Micturition reflex activity in a 1-day-old rabbit. 1, Cystometrogram in intact rabbit; 2, cystometrogram after complete transection of mid-thoracic portion of spinal cord; 3, cystometrogram after suction ablation of lumbo-sacral portion of the spinal cord. There is persistence of organized reflex response of the bladder after complete neurological isolation.